SI of

A theoretical design of chiral molecules through conformational lock towards circularly polarized photoluminescence

Lewen Wang,[a] Tengfei He,[b] Hailiang Liao,[a] Yige Luo,[a] Wen Ou,[a] Yinye Yu,[acd] Wan Yue,[a] Guankui Long,[b*] Xingzhan Wei,[c] Yecheng Zhou[a*]

[a] Guangzhou Key Laboratory of Flexible Electronic Materials and Wearable Devices, School of Materials Science and Engineering, Sun Yat-sen University, Guangzhou 510006, China

[b] School of Materials Science and Engineering, National Institute for Advanced Materials, Renewable Energy Conversion and Storage Center (RECAST), Nankai University, 300350, Tianjin, China

[c] Micro-nano Manufacturing and System Integration Center, Chongqing Institute of Green and Intelligent Technology, Chinese Academy of Sciences, Chongqing 400714, China.

[d] University of Chinese Academy of Sciences, No. 19A Yuquan Road, Shijingshan District, Beijing 100049, China

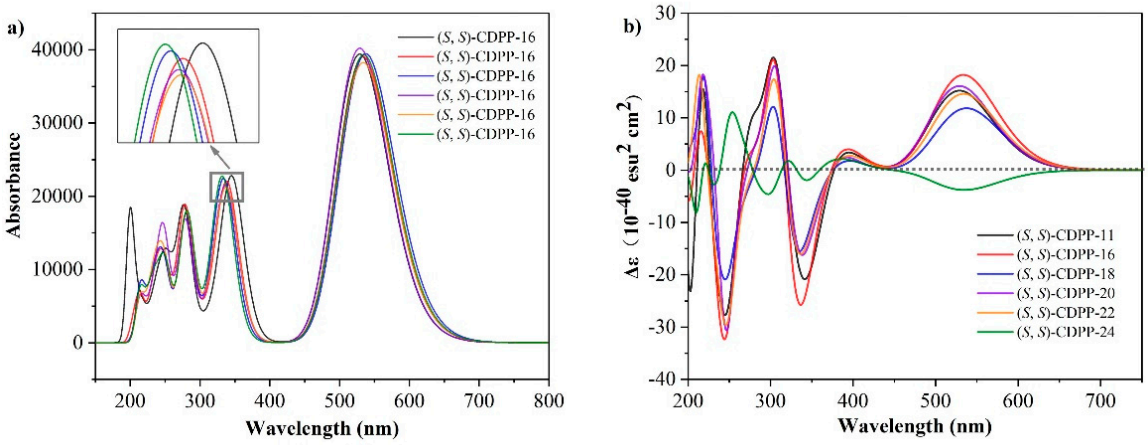

Figure S1. a) Calculated absorption spectrum of (*S*, *S*)-CDPP molecules, b) Calculated ECD spectrum of (*S*, *S*)-CDPP molecules.

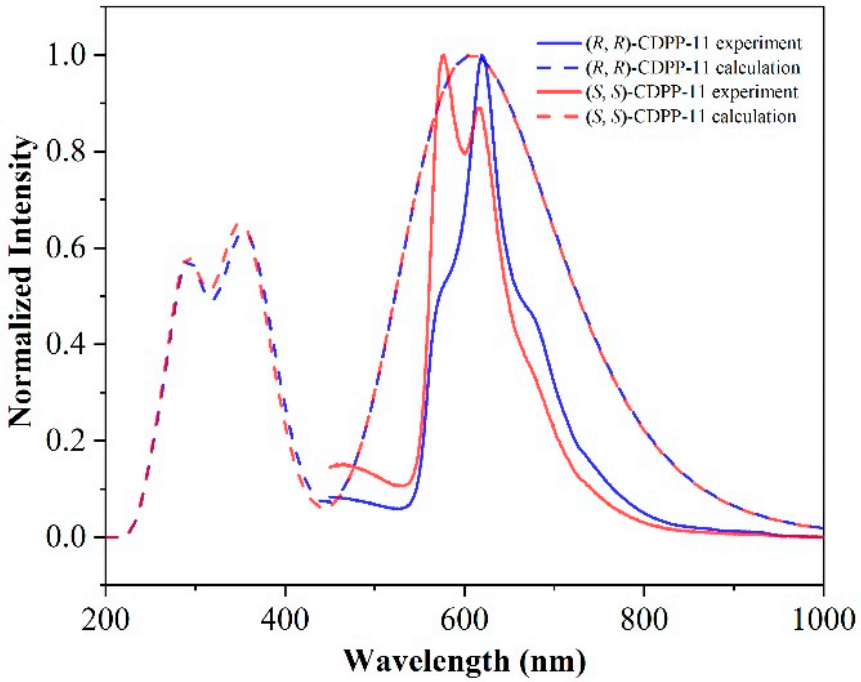

Figure S2. Comparison between the experimental and calculated normalized emission spectrum of CDPP-11.

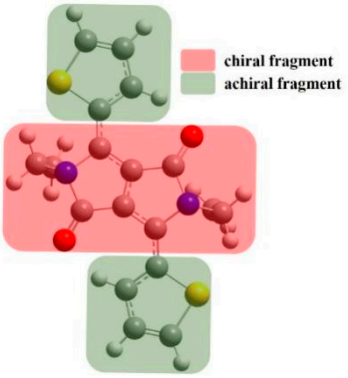

Figure S3. The chiral and achiral fragments of the DPP plane.

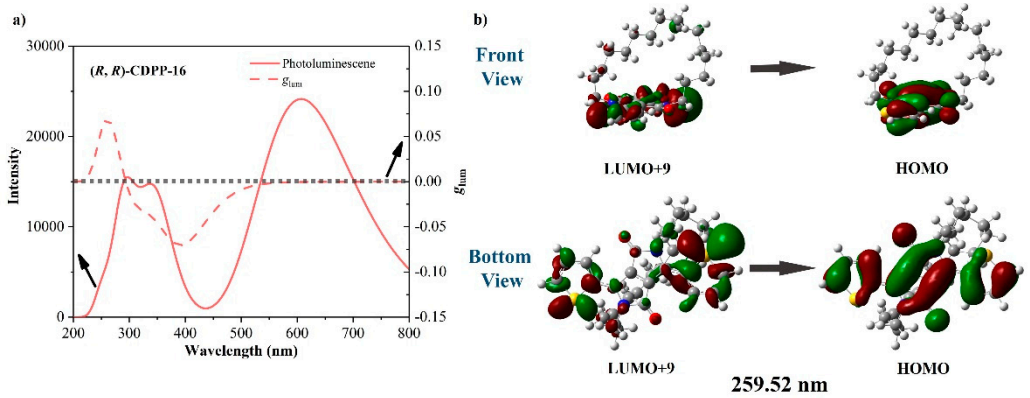

Figure S4. a) Calculated g_{lum} (after Gaussian broadening) and emission spectrum of (*R*, *R*)-CDPP-16, b) The contour surfaces of FMOs involved in the emission peak of (*R*, *R*)-CDPP-16 at 359.52 nm.

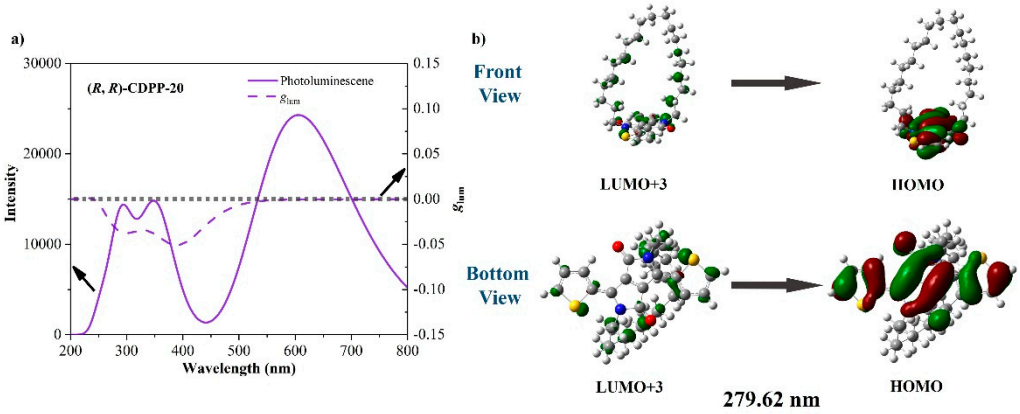

Figure S5. a) Calculated g_{lum} (after Gaussian broadening) and emission spectrum of (*R*, *R*)-CDPP-20, b) The contour surfaces of FMOs involved in the emission peak of (*R*, *R*)-CDPP-20 at 279.62 nm.

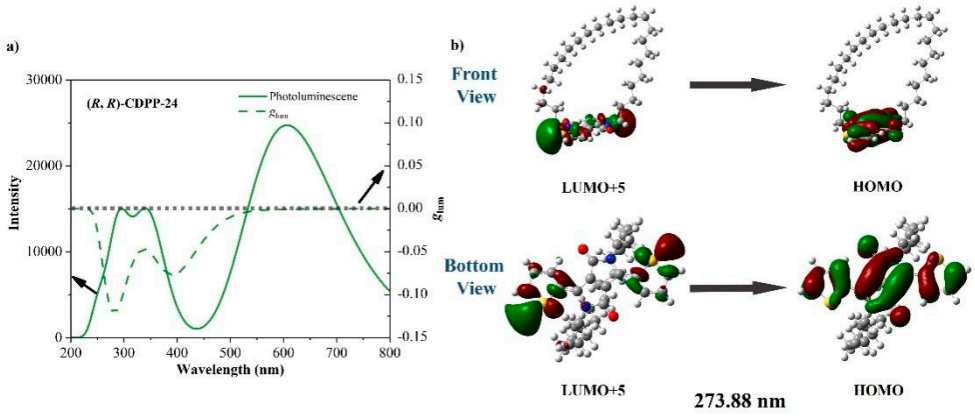

Figure S6. a) Calculated g_{lum} (after Gaussian broadening) and emission spectrum of (*R*, *R*)-CDPP-24, b) The contour surfaces of FMOs involved in the emission peak of (*R*, *R*)-CDPP-24 at 273.88 nm.

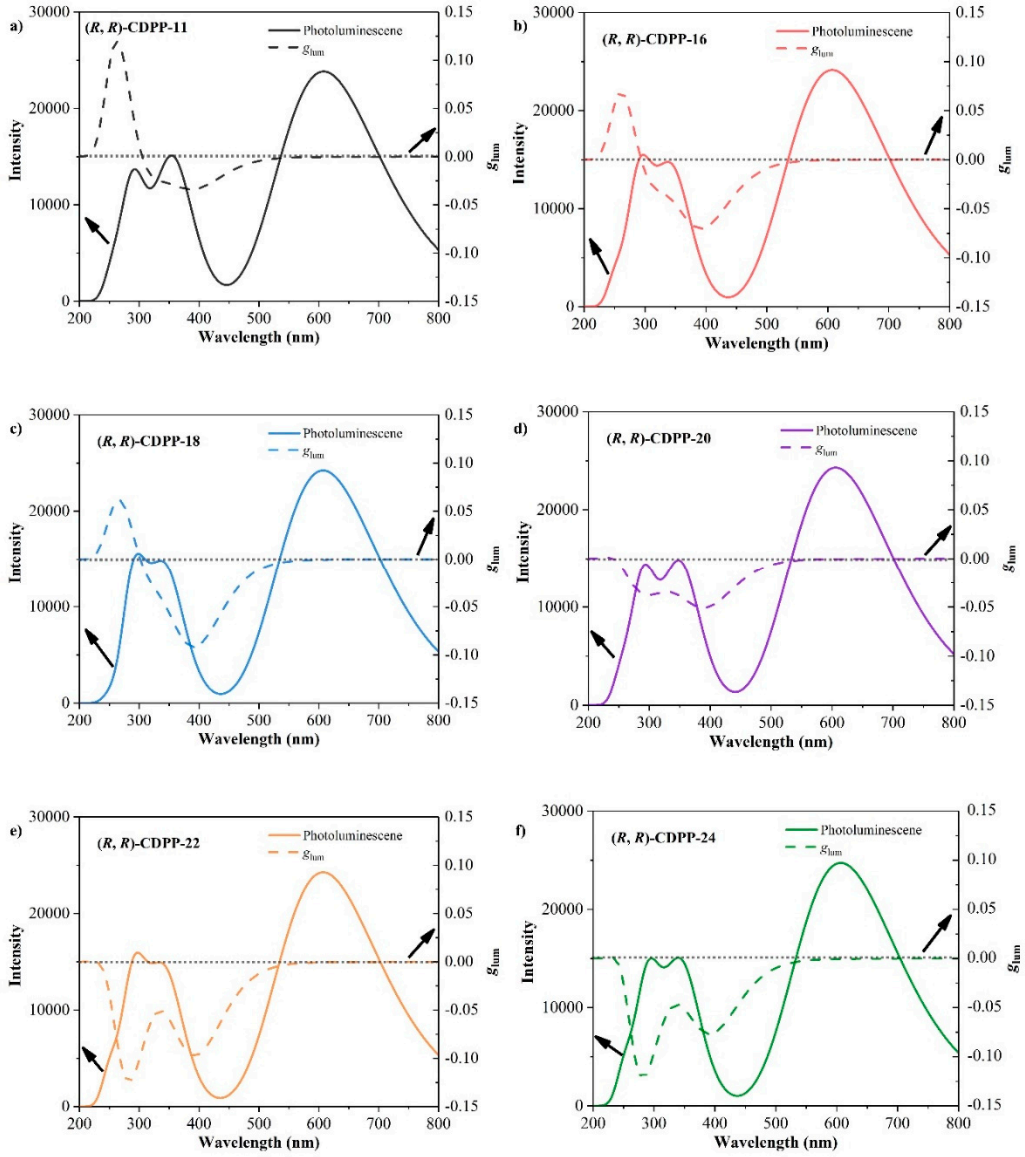

Figure S7. a) Calculated g_{lum} (after Gaussian broadening) and emission spectrum of (*R*, *R*)-CDPP-11, b) Calculated g_{lum} (after Gaussian broadening) and emission spectrum of (*R*, *R*)-CDPP-16, c) Calculated g_{lum} (after Gaussian broadening) and emission spectrum of (*R*, *R*)-CDPP-18, d) Calculated g_{lum} (after Gaussian broadening) and emission spectrum of (*R*, *R*)-CDPP-20, e) Calculated g_{lum} (after Gaussian broadening) and emission spectrum of (*R*, *R*)-CDPP-22, f) Calculated g_{lum} (after Gaussian broadening) and emission spectrum of (*R*, *R*)-CDPP-24.

- **Table S1**. The orbital composition analysis of (*R*, *R*)-CDPP by Hirshfeld method in Multiwfn.

		DPP-Plane		Carbon Chain (%)
		chiral fragment (%)	achiral fragment (%)	
(*R*, *R*)-CDPP-11	**LUMO**	51.235	48.238	0.527
	HOMO	63.821	35.793	0.385
	HOMO-1	80.475	15.591	3.934
	HOMO-8	9.479	0.613	89.9
(*R*, *R*)-CDPP-16	**LUMO+9**	15.58	52.609	31.8
	HOMO	65.255	34.466	0.28
(*R*, *R*)-CDPP-20	**LUMO+3**	23.519	36.478	40
	HOMO	64.443	35.42	0.14
(*R*, *R*)-CDPP-24	**LUMO+5**	6.201	30.225	63.6
	HOMO	64.964	34.934	0.1

- **Table S2**. The proportion change of orbital composition on chiral centers during emission at around 270 nm. The chiral part includes the chiral fragment in DPP plane, and the alkyl chain.

	Transition Path	Orbital composition on chiral centers before transition (%)	Orbital composition on chiral centers after transition (%)	Proportion change (%)
(*R*, *R*)-CDPP-11	LUMO→HOMO-8	51.762	99.390	47.628
(*R*, *R*)-CDPP-16	LUMO+9→HOMO	47.380	65.535	18.155
(*R*, *R*)-CDPP-20	LUMO+3→HOMO	63.519	64.583	1.064
(*R*, *R*)-CDPP-24	LUMO+5→HOMO	69.801	65.064	-4.737

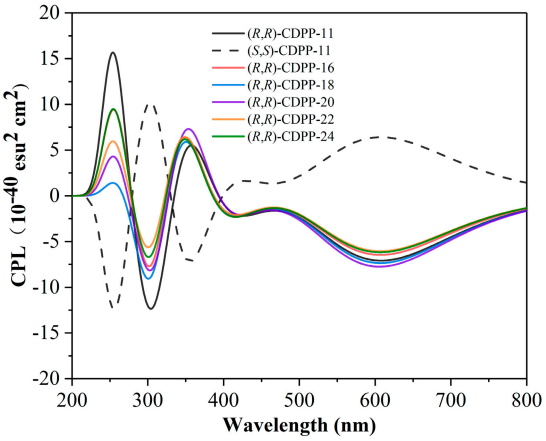

Figure S8. Calculated CPL spectrum of (*R*, *R*)-CDPPs and (*S*, *S*)-CDPP-11.

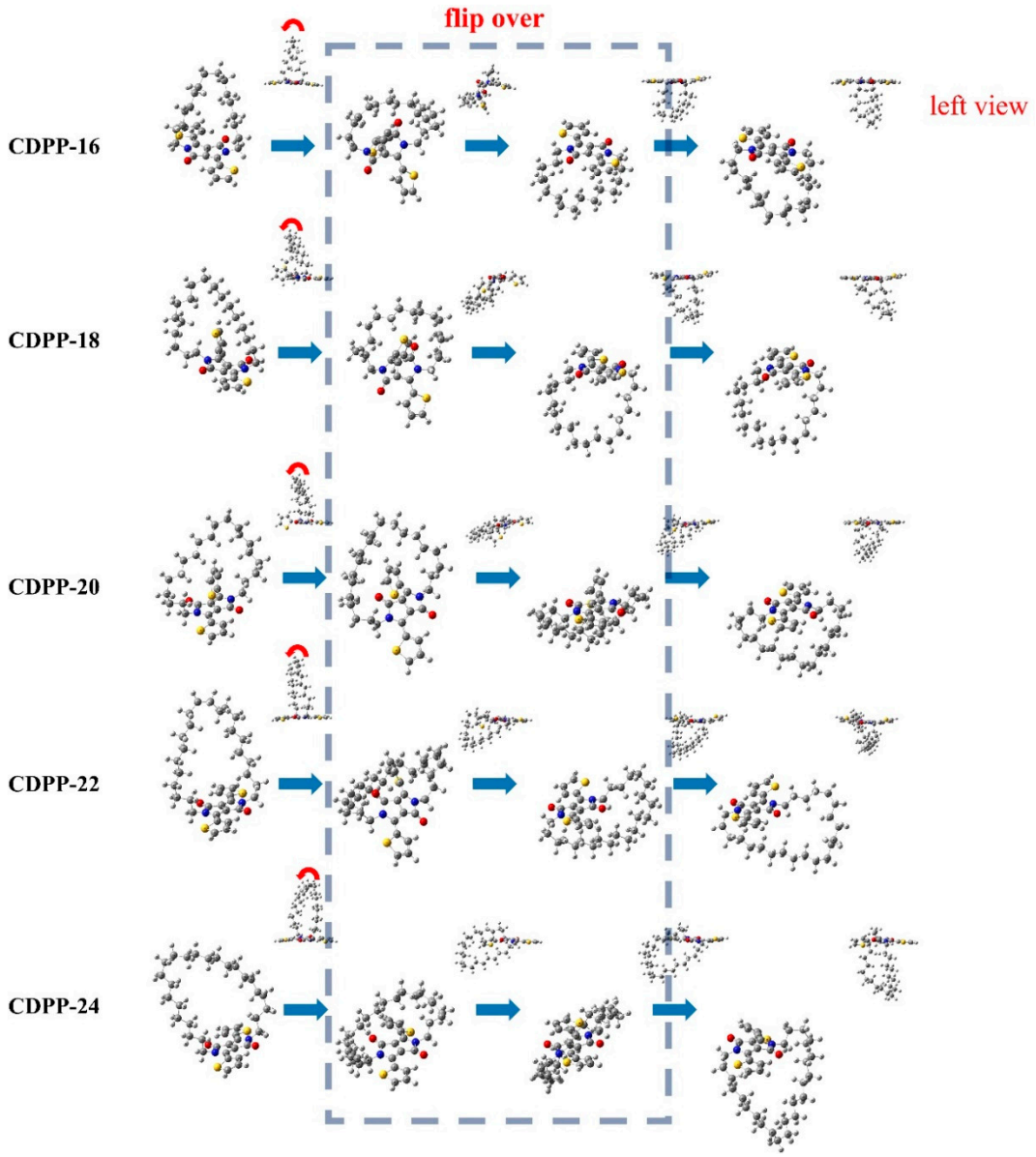

Figure S9. Geometry deforming of CDPP during the flip.

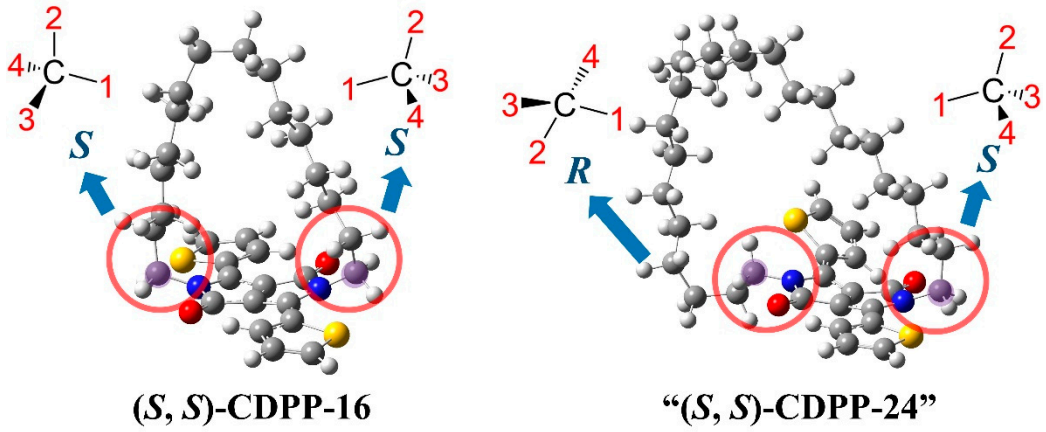

Figure S10. The invalidated conformational lock of "(*S*, *S*)-CDPP-24".

Experimental details of CDPP-11

1.Materials preparation and Optical characterization

Solvents used in experiment were purchased from Sigma Aldrich and were of spectroscopic grade. Silica gel (General-Regent, 200-300 mesh) was used to purify the monomers.

UV−vis absorption spectra were characterized on a UV-1601 Shimadzu UV−vis spectrometer. CD spectra were characterized on a J-810 Circular dichroism spectrometer. Emission spectra were characterized on a fluorescence spectrometer from Hitachi F-6000.

2. Synthesis of DPP

Sodium (3.79 g, 0.17 mol) was added to a stirring solution of methylbutan-2-ol (100.0 ml), then heated to reflux until the sodium was completely dissolved. After the solution was cooled to 100°C, thiophene-2-carbonitrile (10 ml, 0.11 mol) was added, and then dimethyl succinate

(4.9 ml, 0.04 mol) was added dropwise to the solution. After the solution was kept at 100°C and stirred overnight, it was cooled to room temperature. A mixed solution of glacial acetic acid (30 ml)/methanol (40 ml) was added to stop the reaction, and the mixed solution was stirred at 90°C for 10 minutes. The precipitate was collected by filtration and washed several times with water and methanol. Finally, 3,6-bis(6-bromopyridin-2-yl)pyrrole[3,4-c]pyrrole-1,4(2H,5H)-dione product was obtained with a yield of 23.6%. The synthetic route is shown in Figure S11.

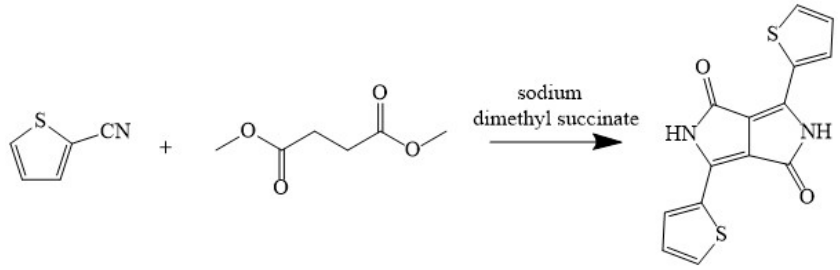

Figure S11. The synthesis of DPP derivative.

3. Synthesis of CDPP-11

After being roasted at 150 °C for 30 min, Potassium carbonate (700 mg, 5 mmol) was cooled to room temperature. DPP (500 mg, 1.66 mmol), 1,11-dibromoundecane (782 mg, 2.49 mmol) and 18-crown-6 (438 mg, 1.66 mmol) were slowly added to 20 ml of anhydrous DMF solution under nitrogen atmosphere. The solution was stirred at 100°C overnight. The solution was cooled to room temperature and 100 ml of deionized water was added, the solution was then stirred for 30 minutes. Another 100 ml portion of deionized water was added and the mixture was extracted with DCM (4×100 ml). The combined organic phases were washed with 200

ml of water and dried over magnesium sulfate. The solvent was removed under reduced pressure. Silica gel chromatography, with hexane:dichloromethane (3:2) as eluent, isopropanol recrystallization to obtain CDPP-11. The synthetic route is shown in Figure S12.

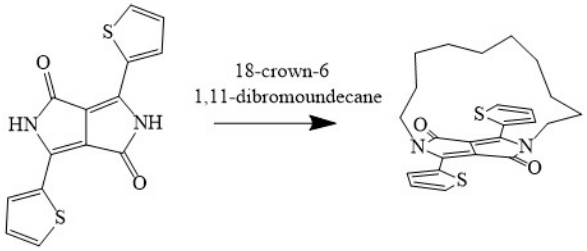

Figure S12. The synthesis of CDPP-11.